Available online at www.sciencedirect.com
ScienceDirect
Journal of Environmental Sciences 2011, 23(9) 1578–1584
JOURNAL OF ENVIRONMENTAL SCIENCES
ISSN 1001-0742
CN 11-2629/X
www.jesc.ac.cn

# Silver impregnated carbon for adsorption and desorption of elemental mercury vapors

Despina Karatza[1], Marina Prisciandaro[2,*], Amedeo Lancia[1], Dino Musmarra[3]

*1. Dipartimento di Ingegneria Chimica, Università di Napoli "Federico II", P. leTecchio 80, 80125 Napoli, Italy. E-mail: karatza@irc.na.cnr.it*
*2. Dipartimento di Chimica, Ingegneria Chimica e Materiali, Università de L'Aquila, Zona Industriale di Pile, Pile, 67100 L'Aquila, Italy*
*3. Centro Interdipartimentale di Ricerca in Ingegneria Ambientale, Dipartimento di Ingegneria Civile, Seconda Università degli Studi di Napoli, Real Casa dell'Annunziata, Via Roma 29, 81031 Aversa (CE), Italy*

Received 06 July 2010; revised 02 March 2011; accepted 12 April 2011

**Abstract**

The $Hg^0$ vapor adsorption experimental results on a novel sorbent obtained by impregnating a commercially available activated carbon (Darco G60 from BDH) with silver nitrate were reported. The study was performed by using a fundamental approach, in an apparatus at laboratory scale in which a synthetic flue gas, formed by $Hg^0$ vapors in a nitrogen gas stream, at a given temperature and mercury concentration, was flowed through a fixed bed of adsorbent material. Breakthrough curves and adsorption isotherms were obtained for bed temperatures of 90, 120 and 150°C and for $Hg^0$ concentrations in the gas varying in the range of 0.8–5.0 mg/m$^3$. The experimental gas-solid equilibrium data were used to evaluate the Langmuir parameters and the heat of adsorption. The experimental results showed that silver impregnated carbon was very effective to capture elemental mercury and the amount of mercury adsorbed by the carbon decreased as the bed temperature increased. In addition, to evaluate the possibility of adsorbent recovery, desorption was also studied. Desorption runs showed that both the adsorbing material and the mercury could be easily recovered, since at the end of desorption the residue on solid was almost negligible. The material balance on mercury and the constitutive equations of the adsorption phenomenon were integrated, leading to the evaluation of only one kinetic parameter which fits well both the experimentally determined breakthrough and desorption curves.

**Key words**: mercury; carbon; MSW incinerators; adsorption; desorption; silver nitrate

**DOI**: 10.1016/S1001-0742(10)60528-1

**Citation**: Karatza D, Prisciandaro M, Lancia A, Musmarra D, 2011. Silver impregnated carbon for adsorption and desorption of elemental mercury vapors. Journal of Environmental Sciences, 23(9): 1578–1584

## Introduction

Mercury is present in the combustion flue gas either as elemental mercury ($Hg^0$), or in the oxidized form as mercuric oxide (HgO), mercuric chloride ($HgCl_2$) and mercurous chloride ($Hg_2Cl_2$) (Ghorishi and Gullett, 1998). In flue gas from municipal solid waste (MSW) incinerators mercury is mainly found as $HgCl_2$ (Pacyna et al., 2006) since there is a relatively high concentration of HCl; while elemental mercury is the prevailing form in emissions from coal combustion processes, due to the reducing properties of $SO_2$ (Pacyna et al., 2006; Schager, 1990).

Among mercury removal treatments, the advantage of dry adsorption processes is that they do not bring about the problem of treatment and stabilization of the waste liquid streams; therefore they seem very attractive for coal combustors and hazardous/municipal waste incinerators. Moreover, mercury control devices must account for differences in system specific concentration and speciation ($Hg^0$ or $Hg^{2+}$). The best available technology (BAT) to reduce these emissions is considered to be fabric filters in combination with dry or wet adsorption methods (European Commission, 2003). Particularly, activated carbon adsorption is a technology that offers a great potential for the control of gas-phase mercury emissions (Yan et al., 2004). However dry adsorption, although being considered more environmental friendly than the wet process, has the disadvantage of the need for exhaust solid disposal. Therefore, the possibility of realizing an adsorption process followed by a desorption unit with the consequent sorbent recovery, appears to be very interesting.

In the last two decades, the need to develop effective mercury control technologies and the attractive features of adsorption processes led researchers to focus their efforts on the evaluation of the adsorption kinetics and sorbent capacity of many different solid sorbents, particularly activated carbons (ACs). It has been demonstrated that several factors potentially affect the efficiency of these sorbents in mercury removal from flue gas; these include the mercury speciation in flue gas; the flue gas composition and process conditions (e.g., flue gas temperature, particulate control

* Corresponding author. E-mail: marina.prisciandaro@univaq.it

equipment). These studies showed that: the elemental mercury is more difficult to beadsorbed than the oxidized form (Schager, 1990; Chang and Offen, 1995; Karatza et al., 1996a,1996b); the sorbent adsorption capacity spans over a wide range by changing the ACs (Ghorishi and Gullett, 1998; Yan et al., 2004; Karatza et al., 1996a, 1996b), and in general, the lower the temperature and $SO_2$ concentration the higher the adsorption capacity (Gullett and Jozewicz, 1993; Krishnan et al., 1994; Karatza et al., 2000; Presto and Granite, 2007).

Moreover, studies devoted to reach a deeper insight of adsorption phenomena onto different ACs, often opportunely modified to increase their adsorption capacity, suggest the following: the higher the specific surface the higher the adsorption capacity (Yan et al., 2004), oxygen surface complexes, lactone and carbonyl groups, are the favourite active sites for $Hg^0$ capture (Li et al., 2003), some additives e.g., $Na_2S$, $CuCl_2$, $Co_3O_4$, $MnO_2$ and $CuCoO_4$, added to the carbon by impregnation process, may have a positive effect on the metal mercury capture (Karatza et al., 2003; Lee et al., 2008; Mei et al., 2008).

Despite the large amount of work has been conducted to evaluate the best operating conditions to capture the mercury present in the flue gas, the kinetic and thermodynamic values which characterize adsorption are scarce, and the studies on mercury desorption by exhaust sorbents are lacking. It is worth noticing that mercury desorption is relevant either to recover the mercury and to detoxify the adsorbing material in order to avoid its stabilization before landfilling or to allow its reuse.

The main goal of the present article is then to investigate the elemental mercury adsorption and desorption behaviors by using a silver nitrate impregnated carbon, with the aim of determining the adsorption and desorption mechanism with kinetic and thermodynamic parameter estimation.

## 1 Materials and methods

Experiments were performed using the laboratory scale apparatus shown in Fig. 1. In this apparatus the gas stream at the required temperature and $Hg^0$ concentration was produced, and the capture of mercury vapors, on a fixed bed of adsorbent material, was performed.

The gas stream was obtained by evaporating liquid mercury contained in a thermo stated glass saturator into a stream of pure nitrogen. The saturator was made of a horizontally placed string of 10 empty glass spheres with 30 mm ID, connected by short and narrow glass tubes (about 1 mm ID, 5 mm in length), into which about 350 g of liquid mercury (reagent grade $Hg^0$ from BDH Inc., Canada) were deposited. This device allowed both a relatively large gas-liquid contact area (over the spheres) and a good mixing of the gas (in the tubes). The mass flow rate of nitrogen into the saturator was kept constant by a hot wire flow rate controller, and the $Hg^0$ concentration in the gas stream fed to the reactor was controlled by varying the temperature of the saturator and by diluting the saturated stream in the junction with a stream of pure nitrogen, the flow rate of which was controlled by another hot wire flow rate controller. The diluted stream was fed to a glass reactor containing sorbent. The reactor was 35 mm ID and 60 mm high, and was kept in a thermostated oven equipped with a PID temperature controller. The

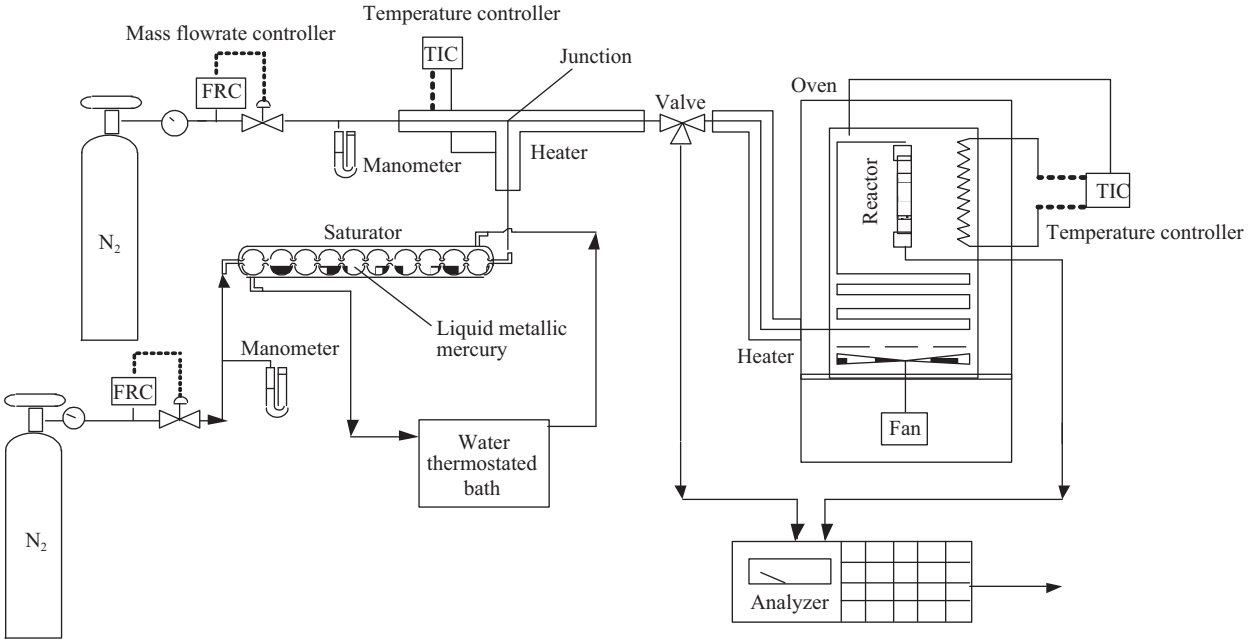


**Fig. 1** Sketch of the experimental apparatus.

adsorbing bed was made of 0.015 g of adsorbing particles mixed with 3.0 g of 100 μm glass beads as inert, and its length was 4 mm. This arrangement was chosen with the aim of avoiding channeling while keeping a small reactive surface. Furthermore, to avoid losses of powder in the gas stream, a downward flow was used in the reactor. Activated carbon impregnated with silver nitrate was used as sorbent. Mercury adsorption results obtained with this untreated carbon are exhaustively reported elsewhere (Karatzaet al., 1996a). The impregnation of the carbon was obtained by sinking the raw activated carbon into 30% (*W*/*W*) aqueous solutions of $AgNO_3$ and then by drying the filtered solid. The resulting $AgNO_3$ concentration over the solids was 40% (*W*/*W*). The bed material properties prior and after the impregnation are reported in Table 1. Preliminary tests (absorbing the outlet gas in aqueous solution with diluted nitric acid) have shown that oxidized mercury is absent, therefore mercury oxidizing reactions do not occur and the mercury is present in the elemental form ($Hg^0$) only.

**Table 1** Darco G60 bed material properties

| | Darco G60 without impregnation* | Darco G60 with $AgNO_3$ impregnation |
|---|---|---|
| Bulk density (kg/m$^3$) | 450 | 728 |
| Average diameter (m) | 3.50 | 3.93 |
| BET surface area (m$^2$/g) | 230 | 183 |

* Karatza et al., 1996a.

Adsorption and desorption experiments were conducted at different temperatures (*T*) of the fixed bed and at different $Hg^0$ concentrations in the inlet stream fed to the bed ($C_0$), while the gas-solid relative velocity was fixed in all runs. In particular, $C_0$ ranged from 0.8 to 5.0 mg/m$^3$ and three temperatures were investigated: 90, 120, and 150°C, while the gas flow rate was kept at about 7.22 $\times10^{-5}$ Nm$^3$/sec, which corresponds to a gas superficial velocity of 7.52$\times10^{-2}$ m/sec. The adsorption experiments were performed using fresh solids and were protracted until the outlet mercury concentration became equal to the inlet concentration. At this time the bed material is at thermodynamic equilibrium with the gas phase and no more mercury is transferred from gas to solid phase. These conditions were kept constant for about an hour, then the inlet mercury concentration was set to zero and desorption of the mercury adsorbed on the bed began. Desorption conditions were continued until the outlet mercury concentration approached zero. Additional runs were performed to evaluate the gas-solid adsorption isotherms; these runs were performed in the same way as adsorption runs but they were stopped before starting desorption, i.e. when gas and solids reach the thermodynamic equilibrium.

The $Hg^0$ concentration in the outlet gas stream from the reactor was determined as a function of time, by using the mercury continuous analyzer MONITOR 2000 by Seefelder Messtechnik (Germany). After each run the mercury on the bed material was measured by leaching the solids with aqua regia ($HNO_3$ + 3HCl) and then analyzing the solution by means of Cold Vapor Atomic Absorption (CVAA, Quantitech Ltd., England), using $NaBH_4$ as reducing agent. A difference not larger than 8% was found in the mercury material balance.

## 2 Results

Figure 2 presents the adsorption and desorption experimental results at 90, 120, and 150°C. The mercury outlet concentration, experimentally measured, in the adsorption and desorption runs versus time is shown in Fig. 2. For the sake of clarity, $t_a$ stands for adsorption time and $t_d$ stands for desorption time. The outlet mercury concentration, referred to the adsorption run, is reported in dimensionless form ($C_{out}/C_0$) as the ratio between the outlet and the inlet mercury concentration (breakthrough curves). Similarly the outlet mercury concentration, referred to the desorption run, is reported as $C_{out}/C_0$, in this case $C_0$ is the gas concentration used to saturate the bed. Data in Fig. 2a refer to runs performed keeping the bed temperature constant at 90°C and using two different values of inlet gas concentration: 0.78 and 4.73 mg/m$^3$. The mercury outlet concentration continuously increases with time approaching the saturation ($C_{out}/C_0$ = 0.95) in a time ($t_s$) which depends on $Hg^0$ concentration in the gas phase. In particular, with increasing $Hg^0$ concentration in the gas phase from 0.78 to 4.73 mg/m$^3$, $t_s$ varies from 0.46 to 0.10 hr. The amount of mercury adsorbed per unit of carbon ($\omega_s$) calculated at $t_s$, is very large in comparison with other sorbents (Seigneur et al., 2004; Karatza et al., 2000) and with the same untreated carbon (Karatza et al., 1996a), and it also depends on $C_0$ being $\omega_s$ = 0.0019 for $C_0$ = 0.78 mg/m$^3$, and $\omega_s$ = 0.0032 for $C_0$ = 4.73 mg/m$^3$. The desorption experimental results reported in Fig. 2a, for the corresponding adsorption runs, show that the $Hg^0$ concentration in the gas phase continuously decreases approaching zero ($C_{out}/C_0$ = 0.05) at a time ($t_r$) equal to 0.4 hr for $C_0$ = 0.78 mg/m$^3$ and 0.14 hr for $C_0$ = 4.73 μg/m$^3$, these time is shorter than $t_s$. The amount of mercury remaining over the sorbent, at $t_r$, is close to zero suggesting that all the adsorbed mercury can be easily desorbed.

Results in Fig. 2b, c at 120°C and 150°C are similar to those in Fig. 2a. In particular, at 120°C, $t_s$ is 0.26 hr when $C_0$ is 0.79 mg/m$^3$ and it decreases to 0.09 hr as $C_0$ increases to 4.60 mg/m$^3$; while at 150°C and $t_s$ is 0.14 hr when $C_0$ is 0.77 mg/m$^3$, and it decreases to 0.05 hr as $C_0$ increases to 4.95 mg/m$^3$. The amount of mercury adsorbed by the solids when it approaches the saturation significantly decreases as the temperature increases, in particular at 120°C, $\omega_s$ is equal to 0.0009 and to 0.0018 for the two $Hg^0$ concentrations in the gas phase and it further decreases at 150°C, reaching the values of $\omega_s$ = 0.0003 and of $\omega_s$= 0.0009. The behavior of the material during the desorption runs at 120 and 150°C is similar to that observed at 90°C; in particular, at 120°C $t_r$ is 0.2 hr for $C_0$ = 0.79 mg/m$^3$ and 0.12 hr for $C_0$ = 4.6 mg/m$^3$; while at 150°C $t_r$ is 0.1 hr for $C_0$= 0.77 mg/m$^3$ and 0.05 hr for $C_0$ = 4.95 mg/m$^3$. In the both runs the residual mercury on the solids is practically zero.

As regards for sorbent recovery, these are very encouraging results: the use of an expensive adsorbent material

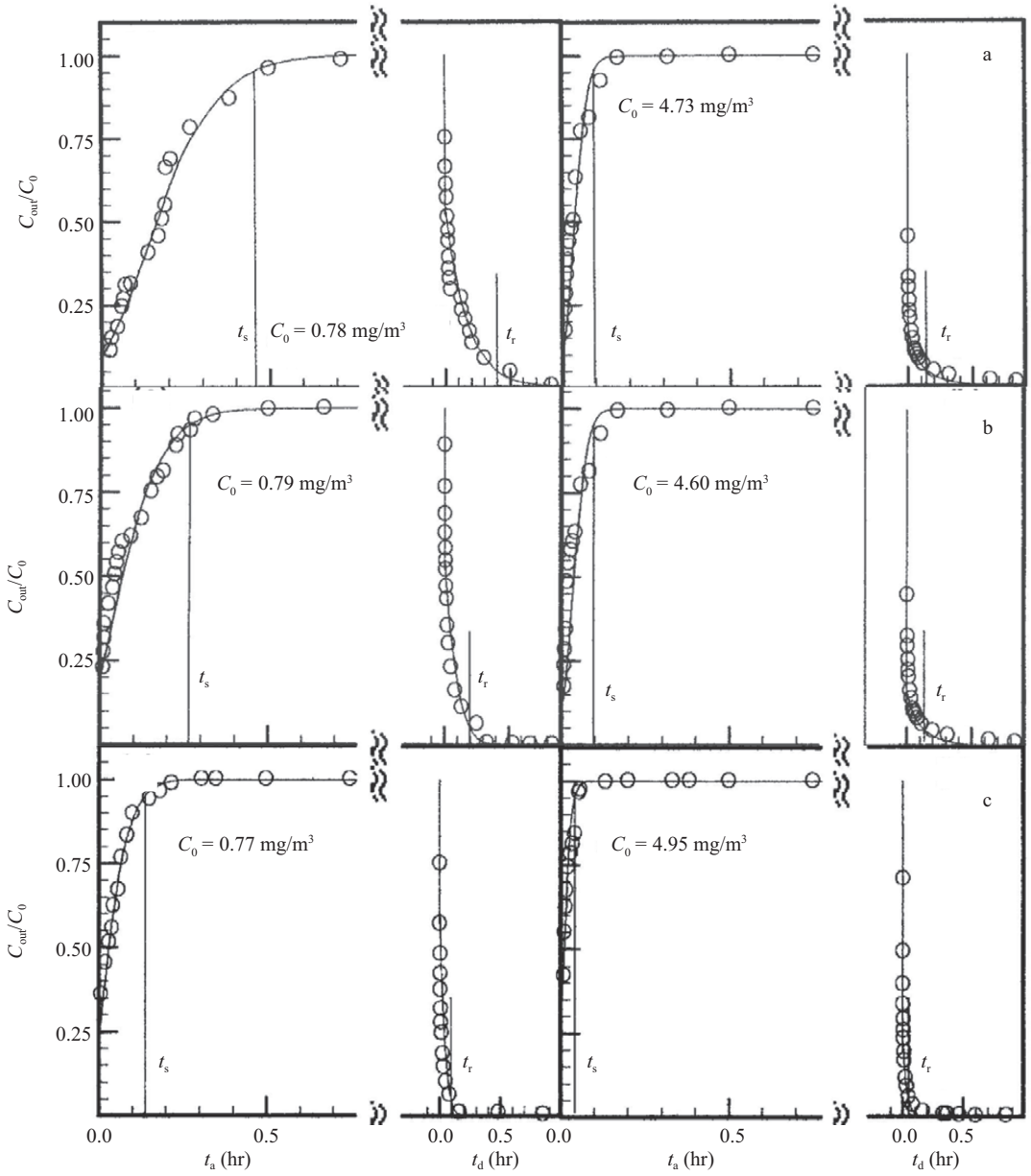


**Fig. 2** Adsorption and desorption experimental runs performed at 90°C (a), 120°C (b), and 150°C (c). $t_a$: adsorption time; $t_d$: desorption time; $t_s$: time for approaching saturation in adsorption runs; $t_r$: time for approaching zero concentration in desorption runs; $C_0$: initial concentration, $C_{out}$: outlet concentration.

such as activated carbon impregnated with silver nitrate, is cost-effective because the sorbent can be re-utilised, since at the end of desorption the residue on solid is almost negligible. It is worth noticing that the desorption mechanism is also very fast if compared to other sorbents. In detail, previous experiments carried out with sulfur impregnated activated carbon at 120°C (Karatza et al., 2000) showed that the $Hg^0$ concentration in the gas phase continuously decreased approaching zero ($C_{out}/C_0$ = 0.05) at a time ($t_r$) equal to about 0.4 hr for two different values of inlet gas concentration (2.24 and 3.93 mg/m$^3$), so from two to four times higher than with respect to the $t_r$ values obtained in the present work with silver nitrate impregnation.

The amount of mercury found on the solid at saturation ($\omega^*$) represents the adsorbate loading in thermodynamic equilibrium with the gas phase at concentration $C^*$. For each temperature, values of $\omega^*$ obtained for different concentrations of the gas stream give the adsorption isotherms.

Figure 3 reports the adsorption isotherms for the three temperatures of 90, 120, and 150°C. These isotherms are of the favorable kind, and they show that the higher the temperature the lower the adsorption capacity, confirming the exothermic nature of the adsorption process under consideration.

By using the well known Langmuir isotherm, the rate of the process can be expressed as the difference between the adsorption rate and the desorption rate therefore the overall rate is expressed by the following Eq. (1):

$$r = k_1(\omega_{max} - \omega)c - k_2\omega \quad (1)$$

where, $c$ (mol/m$^3$) is the $Hg^0$ concentration in the gas phase, $\omega$ (dimensionless) is its concentration as adsorbate on the solid, $\omega_{max}$ is the asymptotic adsorbate concen-

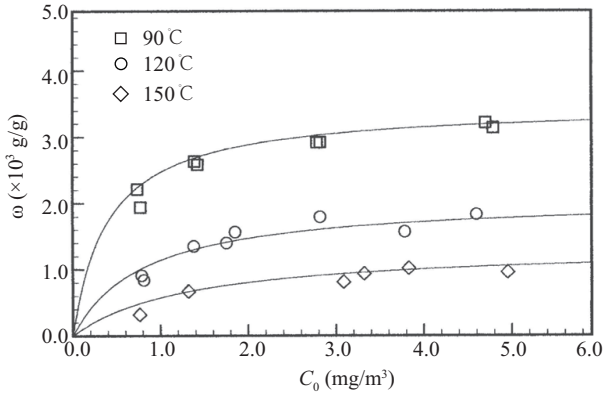


**Fig. 3** Adsorption isotherms for activated carbon impregnated with $AgNO_3$.

tration, and $k_1$ and $k_2$ are the kinetic constants of the adsorption and of the desorption reaction, respectively. At equilibrium ($r = 0$) this rate equation leads to the Langmuir isotherm:

$$\omega^* = \omega_{\max} \frac{Kc^*}{1 + Kc^*} \tag{2}$$

where, $K = k_1/k_2$ is the equilibrium constant.

The equilibrium data of Fig. 4 were used to evaluate the Langmuir parameters as a function of the temperature. Using a nonlinear regression technique these parameters were estimated; all the experimental runs were replicated, so that the experimental error variance could be estimated; the average values are reported in Table 2.

The Langmuir isotherms obtained on the basis of the values of Table 2 are also included in Fig. 3 (continuous lines). The values reported in Table 1 show that both $K$ and $\omega_{\max}$ decrease when temperature increases. In particular, in agreement with the physical meaning of the equilibrium constant $K$, it is possible to hypothesize a dependence on the temperature of the Arrhenius type, according to the following Eq. (3) (Rhee et al., 1986):

$$K = K_0 \exp\left(-\frac{\Delta H_{\text{ads}}}{RT}\right) \tag{3}$$

where, $K_0$ is the pre-exponential factor and $H_{\text{ads}}$ is the heat of adsorption. A nonlinear regression gave the value of 0.531 $m^3/g$ for $K_0$ and the value of –25.4 kJ/mol, which is in the same order of the condensation heat for $Hg^0$, for $\Delta H_{\text{ads}}$.

The values of $K$, together with the continuous line obtained using Eq. (5) with $K_0$ = 0.531 $m^3/g$ and $\Delta H_{\text{ads}}$ = –25.4 kJ/mol, are reported in Fig. 4 in the form of an "Arrhenius" plot.

The values of the kinetic constants $k_1$ and $k_2$ can be evaluated from the experimental breakthrough and desorption data, considering a balance on $Hg^0$ adsorbed in the bed. Indicating the axial coordinate in the bed as $x$ and the time as $t$, it is:

$$V\frac{\partial c}{\partial x} + \varepsilon\frac{\partial c}{\partial t} + \rho_{\text{b}}\frac{\partial \omega}{\partial t} = 0 \tag{4}$$

where, $V$ is the superficial velocity of the gas, $\varepsilon$ is the external void fraction of the bed, and $\rho_{\text{b}}$ is the bulk density of the adsorbent particles. This balance equation must be associated to a constitutive equation for the rate of accumulation on the solid: neglecting the diffusional resistances (see Appendix) and considering Eq. (1), the constitutive equation can be expressed as follows:

$$\frac{\partial \omega}{\partial t} = k_1 (\omega_{\max} - \omega)\, c - k_2 \omega \tag{5}$$

Equations (4) and (5) describe both adsorption and desorption and they have to be integrated subject to the following boundary conditions for the adsorption:

$$\begin{cases} t_{\text{a}} = 0; \quad 0 \le x \le L; \quad c = 0; \quad \omega = 0 \\ t_{\text{a}} \ge 0; \quad x = 0; \quad c = c_0 \end{cases} \tag{6}$$

while for the desorption the boundary conditions are:

$$\begin{cases} t_{\text{d}} = 0; \quad 0 \le x \le L; \quad c = 0; \quad \omega = 0 \\ t_{\text{d}} \ge 0; \quad x = 0; \quad c = c_0 \end{cases} \tag{7}$$

The system of Eqs. (4) and (5) with the boundary conditions (Eqs. (6)–(7)) was solved by using the analytical method proposed by Rhee et al. (1986). Using the experimentally determined values of $K$ and $\omega_{\max}$ for the different temperatures, the $Hg^0$ concentration profiles both in the gas and on the solid phase could be obtained as a function of time. A comparison between the model and the experimental results was possible in terms of $C_{\text{out}}$, which can easily be obtained from the solution of Eqs. (4) and (5). It is important to underline that the only parameter in these equations is $k_1$, which was estimated by fitting model calculations to experimental adsorption and desorption values. Values of $k_1$, together with values of $k_2$, are reported in Table 2. These values are in agreement with the physical meaning of such parameters, indeed they must be independent on the $Hg^0$ inlet concentration to the

**Table 2** Langmuir ($K$, $\omega_{\max}$) and kinetic constants ($k_1$, $k_2$) for Darco G60 activated carbon impregnated with $AgNO_3$

| $T$ (K) | $K$ ($m^3/g$) | $\omega_{\max}$ | $k_1$ ($m^3$/(g·sec)) | $k_2$ ($sec^{-1}$) |
|---|---|---|---|---|
| 363 | 2470 | $3.46 \times 10^{-3}$ | 4.5 | $6.00 \times 10^{-3}$ |
| 393 | 1230 | $2.07 \times 10^{-3}$ | 3.2 | $2.60 \times 10^{-3}$ |
| 423 | 750 | $1.34 \times 10^{-3}$ | 3.0 | $1.21 \times 10^{-3}$ |

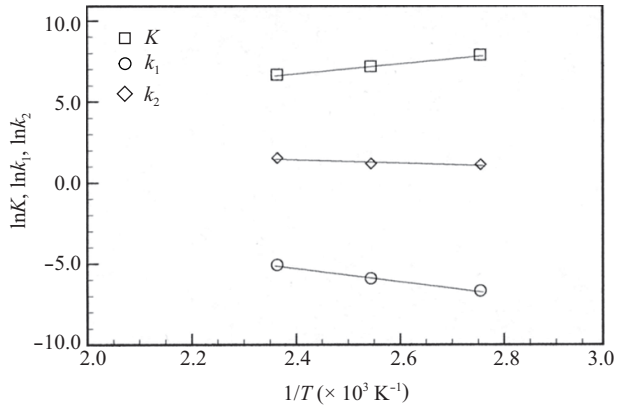


**Fig. 4** Values of thermodynamic and kinetic constants as a function of temperature.

adsorbing bed, while they have to increase (Arrhenius law) with the temperature, and considering the exothermicity of adsorption their ratio have to decrease with temperature. Furthermore, in order to highlight the comparison between model and experimental results adsorption and desorption curves calculated using the values reported in Table 2 are also included in Fig. 2 (continuous lines). This comparison shows that both adsorption and desorption curves well fit the experimental data, this is worth of note considering that a single-parameter model is able to describe adsorption and desorption data.

## 3 Conclusions

The research results presented in this article have been obtained by using a fundamental approach to study the adsorption and desorption of elementary mercury vapors on a commercially available activated carbon (Darco G60 by BDH), impregnated with 40% silver nitrate. Laboratory scale experiments were performed on a fixed bed of adsorbent material; test conditions included variation of $Hg^0$ concentration and of bed temperature. The experimental results showed that such a carbon is very effective to capture elemental mercury and the amount of mercury adsorbed by the carbon decreases as the bed temperature increases. Desorption runs showed that both the adsorbing material and the mercury can be easily recovered, since at the end of the desorption the residue on solid is almost negligible. As to sorbent recovery, these are very encouraging results: the use of an expensive adsorbent material such as activated carbon impregnated with silver nitrate, is cost-effective because the sorbent can be re-used. The study also highlighted that the desorption mechanism is very fast if compared to other sorbents. Eventually, adsorption and desorption curves are properly described by a model based on kinetic control (see Appendix), that has one parameter whose physical meaning is the adsorption kinetic constant.

In conclusion, in this work kinetic and thermodynamic parameters have been obtained. These parameters are essential for the design of a full scale adsorption-desorption unit. It is worth noticing that adsorption and desorption runs have been carried out at the same temperature in order to gain the kinetic constants, but the desorption temperature could be opportunely modified for carbon recovery optimization.

## References


Chang R, Offen G R, 1995. Mercury emission control technologies: an EPRI synopsis. *Power Engineering*, 99: 51–57.

European Commission, 2003. Reference document on best available techniques for large combustion plants. The European Commission, Brussels.

Ghorishi B, Gullett B K, 1998. Sorption of mercury species by activated carbons and calcium-based sorbents: effect of temperature, mercury concentration and acid gases. *Waste Management and Research,* 16: 582–593.

Gullett B K, Jozewicz W, 1993. Bench-scale sorption and desorption of mercury with activated carbon. In: Conference on Municipal Waste Combustion, Williamsburg, VA, USA.

Karatza D, Lancia A, Musmarra D, 2003. Adsorption and desorption of elemental mercury vapors on silver nitrate impregnated carbon, MCS 3. In: 3rd Mediterranean Combustion Symposium, Marrakech, Morocco. 8–13 June.

Karatza D, Lancia A, MusmarraD, Zucchini C, 2000. Study of mercury absorption and desorption on sulfur impregnated carbon. *Experimental Thermal and Fluid Science*, 21: 150–155.

Karatza D, Lancia A, Musmarra D, Pepe F, 1996a. Adsorption of metallic mercury on activated carbon. In: Twenty-Sixth International Symposium on Combustion. The Combustion Institute, Pittsburgh, USA. 2439.

Karatza D, Lancia A, Musmarra D, Pepe F, 1996b. Adsorption of mercuric chloride from simulated incinerator exhaust gas by means of Sorbalit(TM) particles. *Journal of Chemical Engineering of Japan*, 29: 939–946.

Krishnan S V, Gullett B K, Jozevicz W, 1994. Sorption of elemental mercury by activated carbons. *Environmental Science & Technology*, 28: 1506–1512.

Lee S S, Lee J Y, Keener T C, 2008. Novel sorbents for mercury emissions control from coal-fired power plants. *Journal of the Chinese Institute of Chemical Engineers*, 39: 137–142.

Li Y H, Lee C W, Gullett B K, 2003. Importance of activated carbon's oxygen surface functional groups on elemental mercury adsorption. *Fuel*, 82: 451–457.

Mei Z J, Shen Z M, Zhao Q J, Wang W H, Zhang Y J, 2008. Removal and recovery of gas-phase element mercury bymetal oxide-loaded activated carbon. *Journal of Hazardous Materials*, 152: 721–729.

Pacyna E G, Pacyna J M, Fudala J, Strzelecka-Jastrzab E, Hlawiczka S, Panasiuket D, 2006. Mercury emissions to the atmosphere from anthropogenic sources in Europe in 2000 and their scenarios until 2020. *Science of the Total Environment,* 370: 147–156.

Perry R H, Chilton H C, 1973. Chemical Engineers' Handbook (5th ed.). McGraw-Hill, New York.

Presto A A, Granite E J, 2007. Impact of sulfur oxides on mercury capture by activated carbon. *Environmental Science & Technology,* 41: 6579–6584.

Rhee H K, Aris R, Amundson N R, 1986. First Order Partial Differential Equations (Volume I). Prentice-Hall, Englewood Cliffs, USA. 166.

Schager P, 1990. The behavior of mercury in flue gases. Ph. D. Thesis. University of Goteborg, Sweden.

Seigneur C, Vijayaraghavan K, Lohman K, Karamchandani P, Scott C, 2004. Modeling the atmospheric fate and transport of mercury over North America: power plant emission scenarios. *Fuel Processing Technology,* 85: 441–450.

Yan R, Liang D T, Tsen L, Wong Y P, Lee Y K, 2004. Bench-scale experimental evaluation of carbon performance on mercury vapour adsorption. *Fuel*, 83: 2401–2409.

## Appendix

Relative rates of internal diffusion, external diffusion and adsorption itself can be calculated by comparing the experimentally observed relaxation time with the estimated values for the internal and external diffusion time. While from the analysis of the breakthrough curves (Figs. 2–4), it can be derived that the relaxation time is in the order of $10^3$ sec, the two diffusion times can be evaluated as:

$$t_D \cong d/D^2 \quad \text{(A1)}$$

where, $t_D$ is the internal or external diffusion time, $d$ is a characteristic length and $D$ is the appropriate value of the diffusivity. The external diffusion time ($t_{D_{ext}}$) is:

$$t_{D_{ext}} \cong \delta^2/D_{HgCl_2} \quad \text{(A2)}$$

where, $D_{HgCl_2}$ is the gas phase diffusivity of $HgCl_2$ in $N_2$ and δ is the thickness of the external mass transfer boundary layer. As to $D_{HgCl_2}$, Perry and Chilton (1973) reported that the value of $Hg^0$ diffusivity in $N_2$ is $1.3\times10^{-5}$ $m^2$/sec at $T$ = 273 K. Considering an exponent of 1.75 for the dependence on temperature, this corresponds to $D_{Hg^0}$ = $2.8\times10^{-5}$ $m^2$/sec at $T$ = 473 K, a value that can be taken as a fair approximation of the order of magnitude of $D_{HgCl_2}$. In turn $d$ can be estimated from the Sherwood number (Sh) once he Reynolds number (Re) is known. In the present:

$$\mathrm{Re} = GMd_r/S\mu \quad \text{(A3)}$$

where, $M$ is the molar weight of the gas, $d_r$ is the reactor internal diameter, $S$ is the reactor section area and $G$ is the gas viscosity ($G$= $2.3\times10^{-5}$ kg/(m·sec) at $T$ = 150°C and $p$ = 1 atm), so that it is Re = 3.33. Given this low value of Re, it is reasonable to expect Sh = 2, and therefore $\delta = d/2$ = 1.97 μm, which leads to $t_{D_{ext}} \cong 7\times10^{-6}$ sec. As far as the estimation of the internal diffusion time ($t_{D_{int}}$) is concerned, the particle diameter $d$ and the effective intraparticle diffusivity $D_{eff}$ should be used. According to Satterfield and Sherwood the order of magnitude of $D_{eff}$ may be estimated by means of the following equation:

$$D_{eff} = \frac{\varepsilon_p}{\tau}\left(\frac{1}{1/D_{HgCl_2}+1/D_{Kn}}\right) \quad \text{(A4)}$$

where, $\varepsilon_p$ is the internal porosity, defined as the ratio between pore volume and particle volume, $\tau$ is the tortuosity factor and the so called Knudsen diffusivity $D_{Kn}$ (expressed in $cm^2$/sec) can be estimated by means of the following dimensional equation:

$$D_{Kn} = 9.700 r_p \sqrt{T/M_{HgCl_2}} \quad \text{(A5)}$$

where, $M_{HgCl_2}$ is the $HgCl_2$ molecular weight (271.6 g/mol) and $r_p$ (cm)is the effective pore diameter. In turn $r_p$ can be estimated as:

$$r_p = \frac{2\varepsilon_p}{\rho_p s} \quad \text{(A6)}$$

where, $\rho_p$ is the particle density.

The particle density of impregnated Darco G60 can be estimated from its bulk density ($\rho_b$= 728 kg/$m^3$): assuming an external voidage of about 0.5 it is $\rho_p$ = 1456 kg/$m^3$; furthermore, taking the true density of impregnated Darco G60 $\rho_t$ as equal to 3600 kg/$m^3$, it is obtained $\varepsilon_p$=0.60. These two values give $r_p = 2.9\times10^{-7}$cm. In turn from $r_p$ it is obtained $D_{Kn} = 3.7\times10^{-3}$ $cm^2$/sec, and eventually, taking a conservative estimate of $\tau$ = 10, $D_{eff} = 2.2\times10^{-4}$ $cm^2$/sec is obtained which gives $t_{D_{int}} \cong \geqslant \times10^{-4}$ sec.

The comparison between the experimentally evaluated relaxation time (≅ $10^3$ sec) and the two estimated diffusion times (≅$10^{-6}$ sec and ≅$10^{-4}$ sec for the external and the internal diffusion time, respectively) indicates that the rate of the diffusional processes is much bigger than the adsorption rate, and therefore the overall process is controlled by the kinetics of adsorption itself.